J. Am. Soc. Mass Spectrom. (2016) 27:1256–1262
DOI: 10.1007/s13361-016-1393-1

RESEARCH ARTICLE

Reducing Space Charge Effects in a Linear Ion Trap by Rhombic Ion Excitation and Ejection

Xiaohua Zhang,[1] Yuzhuo Wang,[2,3] Lili Hu,[3] Dan Guo,[3] Xiang Fang,[2] Mingfei Zhou,[1] Wei Xu[3]

[1]Department of Chemistry, FUDAN University, Shanghai, 200433, China
[2]National Institute of Metrology, Beijing, 100013, China
[3]School of Life Science, Beijing Institute of Technology, Beijing, 100081, China

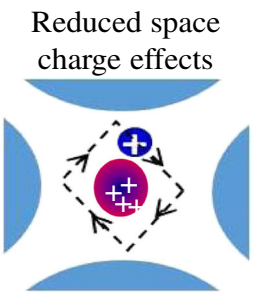

Abstract. Space charge effects play important roles in ion trap operations, which typically limit the ion trapping capacity, dynamic range, mass accuracy, and resolving power of a quadrupole ion trap. In this study, a rhombic ion excitation and ejection method was proposed to minimize space charge effects in a linear ion trap. Instead of applying a single dipolar AC excitation signal, two dipolar AC excitation signals with the same frequency and amplitude but 90° phase difference were applied in the x- and y-directions of the linear ion trap, respectively. As a result, mass selective excited ions would circle around the ion cloud located at the center of the ion trap, rather than go through the ion cloud. In this work, excited ions were then axially ejected and detected, but this rhombic ion excitation method could also be applied to linear ion traps with ion radial ejection capabilities. Experiments show that space charge induced mass resolution degradation and mass shift could be alleviated with this method. For the experimental conditions in this work, space charge induced mass shift could be decreased by ~50%, and the mass resolving power could be improved by ~2 times at the same time.

Keywords: Space charge effects, Rhombic ion excitation, Ion trajectory simulation, Linear ion trap

Received: 22 October 2015/Revised: 16 March 2016/Accepted: 19 March 2016/Published Online: 14 April 2016

Introduction

With ion trapping and mass selective manipulation capabilities, quadrupole ion traps have been used both as stand-alone mass analyzers (especially in mini-MS systems [1–3]) and in hybrid MS [4] instruments for ion storage and/or structure analysis. Compared with beam-type mass analyzers (such as time-of-flight [5] quadrupole rods), an ion trap typically traps a large amount of ions [6–8] (thousands to millions of ions) and an ion cloud is formed in its center [9]. The density and volume of the ion cloud increase as the number of ions increases [10, 11]. With the presence of a large population of ions, ion–ion Coulomb interactions, namely space charge effects, would alter ion motion frequencies in an ion trap [12–14]. During a conventional dipolar ion excitation process for either collision induced dissociation (CID) [8, 15] or ion mass-selective ejection, space charge could also result in delayed ion ejection [16], peak covalence, and nonlinear resonance of excited ions, which is similar to high-order field effects [10, 17–23]. As a result, space charge effects degrade MS performances in terms of dynamic range, mass accuracy, and resolving power [4, 24–33].

A number of methods have been proposed to reduce space charge effects and/or increase ion trapping capacities of quadrupole ion traps. By changing physical geometries of quadrupole ion traps [34], ion trapping volume could be increased, such as the developments of linear ion traps, ion trap arrays, the planar ion trap, the toroidal ion trap, etc. High-order electric fields [35, 36] were also utilized to enhance the ion ejection process and reduce space charge effects. Based on dynamically restricting the total number of ions inside an ion trap, techniques such as dynamic fill time (DFT) and automatic gain control (AGC) have also been applied in commercial MS instruments to minimize space charge effects and increase dynamic range of an ion trap mass analyzer.

In this study, a new ion manipulation method, the rhombic ion excitation and ejection method, was proposed and tested on

Electronic supplementary material The online version of this article (doi:10.1007/s13361-016-1393-1) contains supplementary material, which is available to authorized users.

Correspondence to: Mingfei Zhou; *e-mail:* mfzhou@fudan.edu.cn, Wei Xu; *e-mail:* weixu@bit.edu.cn

a linear ion trap designed with axial ion ejection capability. By applying two dipolar AC excitation signals in both x- and y-directions of a linear ion trap, mass selected ions could be excited to a close to rhombic orbit. In this fashion, excited ions will orbit around the ion cloud trapped at the center of the ion trap, instead of penetrating through the ion cloud during excitation. Therefore, Coulomb interactions between ion cloud and excited ions would be reduced, thus reducing space charge effects. After excitation, ions were ejected axially, and improved mass resolving power and mass accuracy could be observed.

Theoretical

Under the pseudo-potential approximation (with the Mathieu equation coefficient $q<0.4$) and with controlled number of ions [9, 10], an ion cloud trapped in a quadrupole ion trap would have a Gaussian distribution in the direction of the quadrupole electric field. According to the ion distribution model proposed by Guo et al. [37], the electric field generated by the ion cloud within a linear ion trap has an expression of

$$E(r) = \frac{z\rho_l}{2\pi r\varepsilon_0}\left[1-\exp\left(\frac{-r^2}{2a^2}\right)\right] \quad (1)$$

in which z is the electric charge that an ion possesses, ε_0 is the permittivity of vacuum, r is the radical distance to the trap center, a is the standard deviation of Gaussian distribution (which correlates to the physical dimension of the ion cloud), ρ_l is the ion line density, $\rho_l = N/z_0$ and z_0 is the effective length of the linear ion trap.

For the situation of ion penetrating through the ion cloud, modulated ion motion angular frequency would be

$$\omega \approx \sqrt{\omega_0^2 - \frac{z}{m}\left(P_1 + \frac{3P_3a_1^2}{4} + \frac{5P_5a_1^4}{8} + \frac{35P_7a_1^6}{64} + \frac{63P_9a_1^8}{128} + \frac{231P_{11}a_1^{10}}{512}\right)} \quad (2)$$

where m is the mass of an ion, a_1 is the ion motion amplitude, ω_0 is the secular frequency of the ion (angular frequency), P_n ($n=1, 3, 5, 7, 9, 11$) are polynomial coefficients of the electric field function E(r). Details can be found in Guo et al. 2014 [37].

Rhombic ion excitation is more complicated. Given that ion trajectory can be approximated as a circle (see Supplementary Information for details), the ion motion equation can be written as:

$$ma_1\omega^2 = ma_1\omega_0^2 - zE(a_1) \quad (3)$$

and the ion motion angular frequency can be derived from Eq. 3:

$$\omega = \sqrt{\omega_0^2 - \frac{zE(a_1)}{ma_1}} \quad (4)$$

When $2*10^6$ ions ($m/z=195$ Da) are trapped in a linear ion trap, the motion frequencies of a single ion ($m/z=195$ Da) at different motion amplitudes are plotted in Figure 1a. Please note that ion circular motion was used to approximate the ion rhombic motion in Figure 1. Since the space charge force is always pushing ions away from the trap center, decreased ion motion frequencies are observed in both the dipolar ion excitation and the rhombic ion excitation modes. Figure 1b shows the ion secular motion frequency shifts at an ion motion amplitude of 4 mm in both situations under different ion abundances. When applying the rhombic ion excitation, ion motion frequency shift would be smaller than that when applying the dipolar ion excitation.

Both radial and axial ion ejections are based on mass-selective ion excitations in the x-direction and/or y-direction of a linear ion trap. The fringing fields along the z-direction would contribute to pulling ions out of the ion trap when their motional amplitudes (in the x-direction and/or y-direction) are larger than a certain level [23, 38]. Therefore, the smaller frequency shifts (Figure 1) in x-y cross section of the linear ion trap, the reduced space charge effects are expected with the rhombic ion excitation operation. Three-dimensional ion trajectory simulations were also carried out to simulate the ion axial ejection process, and results show that the rhombic ion motion in the x-y plane is the key for reduced space charge effects during an axial ion ejection process (details could be found in Supplementary Information).

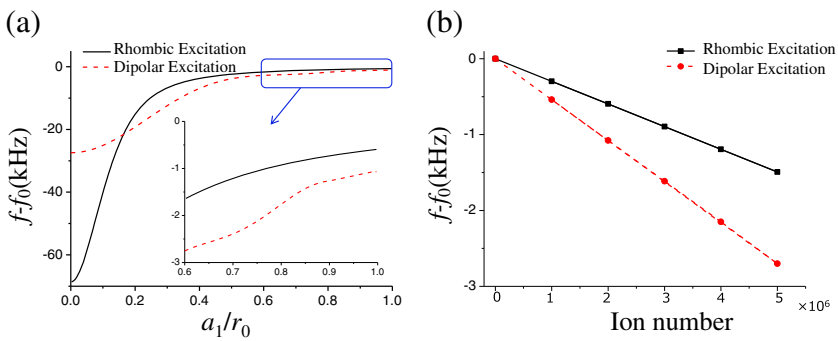

Figure 1. (**a**) Ion secular frequency shifts under different ion motion amplitudes, $N=1\times10^6$; (**b**) Ion secular frequency shifts with different ion abundances at an ion motion amplitude of 4 mm. T = 300 K, m/z = 195 Da, singly charged and the q value in Mathieu Equation equals to 0.36

Experimental

The Linear Ion Trap

A linear ion trap consisting of four identical rod electrodes was designed and constructed as shown in Figure 2. Dimensions of the linear ion trap are as follows: rod length 45 mm; rod radius (r_d) 6 mm; r_0 equals to 5.33 mm. Two circular plate electrodes (thickness: 1 mm; radius: 20 mm) were placed at both ends of the quadrupole rods to serve as the end-cap electrodes. There is a hole (inner radius ~ 2 mm) on each end-cap for ion injection and ejection. These end-caps were placed ~ 3.5 mm away from the quadrupole rods. Since excited ions would rotate inside the ion trap in the rhombic ion excitation mode, they would be more sensitive to high-order fields. Therefore, the high-order field components need to be carefully controlled.

MS Instrumentation

A MS testing platform with a three-stage vacuum chamber was used to host the linear ion trap. Details about the instrument setup could be found in Wang et al. [39]. Briefly, a nano electrospray ionization source was used for sample ionization. Working pressure in the ion trap was maintained around 1 mTorr by introducing N_2 as buffer gas. The electronic control system was developed in-house. Through capacitive coupling, two dual-phase radio frequency (rf) signals (0.87 MHz) and two dipolar alternative current (AC) signals (with stored waveform inverse Fourier transform function, SWIFT) were generated to achieve rhombic ion excitation and ejection. An electron multiplier was placed behind the end-cap electrode of the linear ion trap. After ions were excited to a larger motion radius in the x-y direction, they would feel the fringing electric field and be ejected in the z-direction of the linear ion trap and detected by the electron multiplier [23, 38]. A relationship between the total number of ions trapped in the ion trap with respect to the ion injection time was derived and can be found in the Supplementary Information.

Samples

Polyethylene glycol (PEG 600) and reserpine were purchased from Sigma Aldrich (St. Louis, MO, USA). Electro-sprayed PEG and reserpine were diluted with methanol/water (1:1 v/v) to 100 μg/mL.

Results and Discussions

Conventionally, when a single dipolar AC signal was applied onto a linear ion trap in the x-direction, for instance, excited ions would have an increased sinusoidal secular motion in the x-direction under the pseudopotential approximation [40]. The rest of the trapped ions would form an ion cloud with an ion spatial distribution in both x- and y-directions following the Boltzmann distribution under thermal equilibrium [9, 16, 41, 42]. Therefore, excited ions would penetrate through the ion cloud many times before ejection, and the Coulombic force (or relative distance) between the ion cloud and an excited ion changes with time or the momentary position of the excited ion [10, 17, 19].

In the rhombic ion excitation mode, mass selected ions were excited in both x- and y-directions by two dipolar AC signals. Since the linear ion trap tested in this work is geometrically symmetric in x- and y-directions, the ion motion frequencies in x- and y-directions are also the same. Therefore, two AC signals with the same frequency and amplitudes were applied in the x- and y-directions of the ion trap, respectively. By tuning the phase difference between these two AC signals (Δφ), excited ions could have different trajectories. Ion trajectory simulation results show that a close to rhombic ion trajectory could be obtained with a phase difference of 90° (Figure 3, insets). In the simulation, an ion with *m/z* 195 Da was placed in the linear ion trap, and nitrogen was used as the buffer gas at 1 mTorr. The ion initial positions in both x- and y-directions are set at 0.1 mm in the simulation. Voltage and frequency of the dipolar AC signal are 750 mV and 234 kHz, respectively. The applied rf signal has a voltage of ~200 $V_{0\text{-}p}$ at 0.87 MHz. In this mode, an excited ion would have a spiral

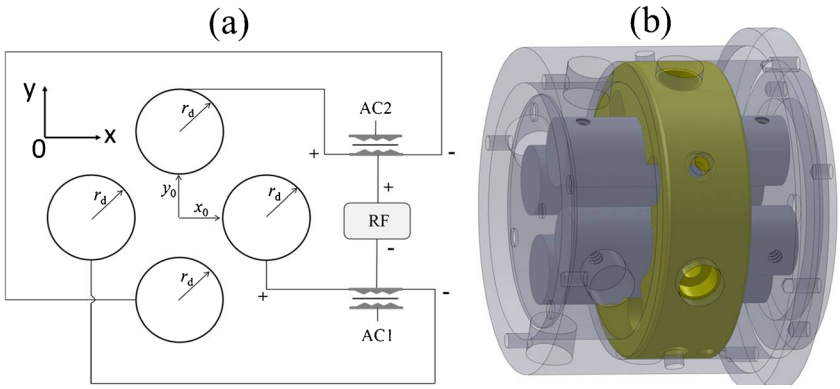

Figure 2. Electric connection (**a**) and structure (**b**) of the linear ion trap. Length of linear ion trap in z-direction is 45 mm, $r_d = 6$ mm and $x_0 = y_0 = r_0 = 5.33$ mm

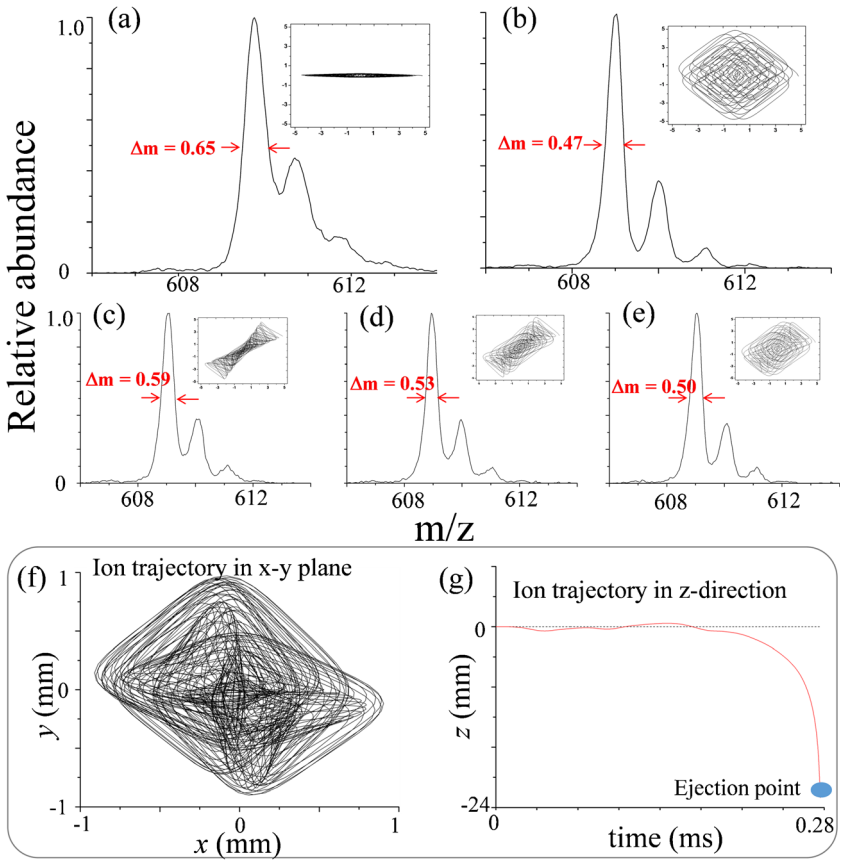

Figure 3. Peak shape and resolution of reserpine under different ion excitation modes. (**a**) Single dipolar AC excitation in x-direction; two dipolar AC excitation (**b**) $\Delta\phi = 90°$; (**c**) $\Delta\phi = 0°$; (**d**) $\Delta\phi = 30°$; (**e**) $\Delta\phi = 60°$. Amplitude and frequency of the AC signals are 500 mV and 210 kHz, respectively. Ion injection time 75 ms. 3D simulation of the ion ejection process (**f**) ion trajectory in x-y plane, (**g**) ion trajectory in z-direction. Insets: simulated ion trajectories under different ion excitation conditions. Buffer gas pressure 1 mTorr (nitrogen). Ion initial positions in both x- and y-directions are set at 0.1 mm

trajectory, and the relative distance between the ion cloud and the excited ion could be close to constant after equilibrium is established. In practice, during the ion axial ejection process, an excited ion also experiences the fringing electric field at the end of the ion trap. With the applied excitation AC signal in the x-y plane, the ion starts to acquire bigger and bigger motional amplitudes in the x-y plane. At the same time, it feels the fringing electric field in the z-direction and drift towards one of the endcaps in the z-direction. With larger motional amplitudes in the x-y plane, the ion feels stronger fringing electric fields in the z-direction, and finally is ejected axially. With conventional single AC excitation, the ion would move up and down in one direction in the x-y plane, and it will pass through the rod-shaped ion cloud in each cycle (please refer to Supplementary Information for details). With rhombic AC excitation, the ion would have a close to rhombic motion in the x-y plane, and it will "circle" around the rod-shaped ion cloud (Figure 3f and g). Therefore, a reduced space charge effect would be observed for rhombic ion excitations. As a result, Coulombic force induced ion motion frequency shift would be smaller in the rhombic excitation mode than in the dipolar excitation mode. Details about the theoretical analysis of space charge induced ion motion frequency shift can be found in Guo et al. [37].

Experiments were then performed to study the effects of $\Delta\varphi$ on minimizing Coulombic interactions within the linear ion trap. As shown in Figure 3a, a full width at half maximum (FWHM) of 0.65 Da was measured for reserpine ions at 609 Da with a relatively long ion injection time (75 ms) using a single dipolar AC excitation signal in the x-direction. Based on ion trajectory simulations, reduced space charge effects are expected with the addition of the second dipolar AC excitation signal in the y-direction. Instead of penetrating through the ion cloud at the trap center, excited ions start to orbit around the ion cloud by increasing $\Delta\varphi$ from 0 to 90°. At the same time, reduced space charge effects and improved mass resolution are observed, and an

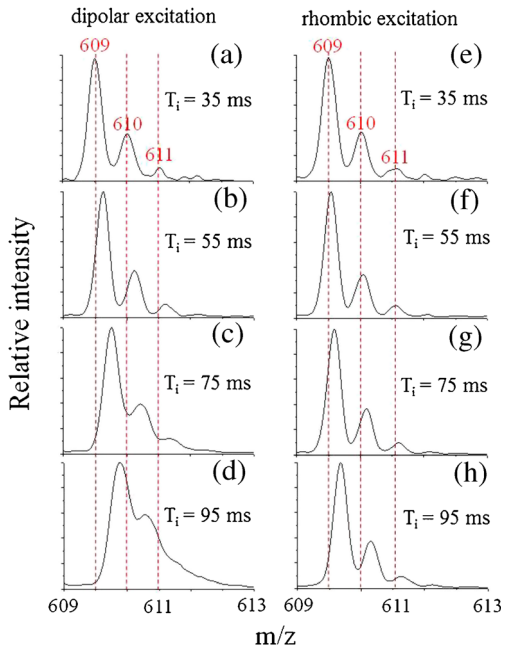

Figure 4. Mass spectra of reserpine at different ion injection times and with different excitation methods. Dipolar excitation with ion injection time: (**a**) 35 ms; (**b**) 55 ms; (**c**) 75 ms; (**d**) 95 ms. Rhombic excitation with ion injection time: (**e**) 35 ms; (**f**) 55 ms; (**g**) 75 ms; (**h**) 95 ms. AC excitation voltage 500 mV, frequency 210 kHz

optimized result is achieved at $\Delta\varphi = 90°$ (FWHM of 0.47 Da). Therefore, this optimized phase difference (90°) was applied in all later experiments.

Effectiveness of this rhombic ion excitation and ejection method on the reduction of space charge effects was first tested using reserpine. Figure 4 plots some typical mass spectra of reserpine at different ion injection times, which corresponds to different numbers of ions. When space charge effects are neglectable (for instance, with ion injection time 35 ms), mass spectrum obtained using rhombic ion excitation is similar to that using conventional dipolar AC excitation. With longer ion injection time, stronger Coulombic interactions can be observed, which are broadened mass peaks and increased mass shifts. It can be observed that this rhombic ion excitation method could effectively reduce the space charge induced mass shift and peak broadening. Figure 5 quantitatively characterizes the reduction of space charge effects. With the help of rhombic ion excitation, ion injection time can be increased from 70 to 105 ms without losing mass resolving power. On the other hand, mass resolving power has a sharp decline with single dipolar AC excitation with an ion injection time from 70 and 105 ms. If we assume a linear relationship between ion injection time and number of ions being trapped, a ~50% increase of ion trapping capacity is expected. Mass shifts can also be effectively reduced, for instance a mass shift of 609.17 Da compared with 609.52 Da with an ion injection time of 75 ms. On the other hand, space charge induced mass shift can be decreased by ~67%, and the mass resolving power can be improved by ~2 times, when space charge effects are strong (for instance, with ion injection time longer than 90 ms).

PEG 600 was also used to further characterize this rhombic ion excitation technique. Different from reserpine, PEG would show a bunch of peaks, which covers a broad mass range (from 300 to 800 Da). In this case, space charge would have stronger effects at the low mass range than those at the high mass range using forward scan, since heavy ions still remained at the center of the trap when light ions were being excited. As shown in Figure 6, the rhombic ion excitation technique could help on both the low mass end and the high mass end in terms of reduced space charge effects. For example, with the help of rhombic ion excitation, the mass shifts reduce from 2.6 to 0.9 Da at *m/z* 437 Da, from 1.9 to 0.7 Da at *m/z* 525 Da, and from 1.0 to 0.0 Da at *m/z* 701 Da, when the ion injection time is set at 105 ms. Rhombic ion excitation also improves mass resolving power of the linear ion trap at different mass ranges with the presence of a large ion populations. With an ion injection time of 105 ms, FWHMs of the mass peaks in PEG

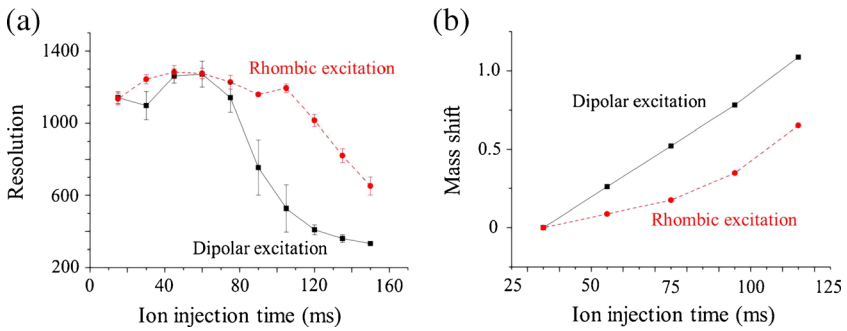

Figure 5. Mass resolution degradations (**a**) and mass shifts (**b**) of reserpine in terms of increased ion injection time. Amplitude and frequency of the AC signals are 500 mV and 210 kHz, respectively

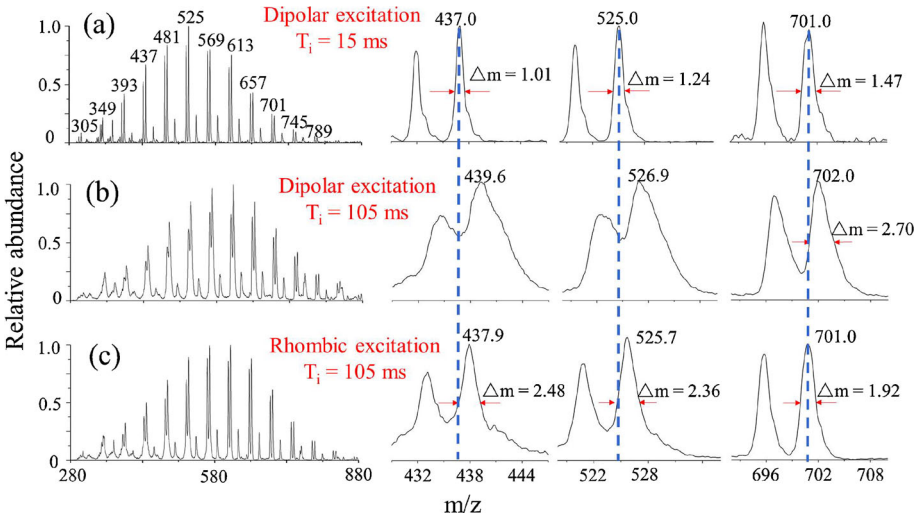

Figure 6. Mass spectra of PEG 600 obtained under different ion injection times and different ion excitation modes. (**a**) Single dipolar ion excitation, ion injection time 15 ms; (**b**) single dipolar ion excitation, ion injection time 105 ms; (**c**) rhombic ion excitation, ion injection time 105 ms. Amplitude and frequency of the AC signals are 500 mV and 210 kHz, respectively. T_i represents ion injection time

600 mass spectra decrease from >5 to 2.48 Da at *m/z* 437 Da, from >5 to 2.36 Da at *m/z* 525 Da, and from 2.7 to 1.92 Da at *m/z* 701 Da.

Conclusions

A new ion excitation and ejection method, the rhombic ion excitation method, was proposed and realized on a linear ion trap. This rhombic ion excitation method could effectively reduce space charge effects by driving excited ions around the ion cloud instead of penetrating through the ion cloud. Two dipolar AC excitation signals with an optimized 90° phase difference were used to excite ions in both the x- and y-directions. This technique could not eliminate space charge effects, but could help alleviate Coulombic interaction induced ion motion frequency shift. As a result, ion trapping capacity of the linear ion trap could be increased by ~50% without losing mass resolving power. This technique could also be applied on top of other space charge control methods, such as AGC and DFT, to maximize the trapping capacity and dynamic range of an ion trap mass analyzer.

Acknowledgments

This work was supported by NNSF of China (21205005, 21475010), 1000 Plan (China), MOST Instrumentation Program (China) (2011YQ0900502 and 2012YQ040140-07).

References

1. He, M., Xue, Z., Zhang, Y., Huang, Z., Fang, X., Qu, F., Ouyang, Z., Xu, W.: Development and characterizations of a miniature capillary electrophoresis mass spectrometry system. Anal. Chem. **87**, 2236–2241 (2015)
2. Zhai, Y.B., Feng, Y., Wei, Y.Z., Wang, Y.Z., Xu, W.: Development of a miniature mass spectrometer with continuous atmospheric pressure interface. Analyst **140**, 3406–3414 (2015)
3. Xu, W., Manicke, N.E., Cooks, G.R., Ouyang, Z.: Miniaturization of mass spectrometry analysis systems. J. Assoc. Lab. Autom. **15**, 433–439 (2010)
4. Makarov, A., Denisov, E., Kholomeev, A., Balschun, W., Lange, O., Strupat, K., Horning, S.: Performance evaluation of a hybrid linear ion trap/orbitrap mass spectrometer. Anal. Chem. **78**, 2113–2120 (2006)
5. Campbell, J.M., Collings, B.A., Douglas, D.J.: A new linear ion trap time-of-flight system with tandem mass spectrometry capabilities. Rapid Commun. Mass Spectrom. **12**, 1463–1474 (1998)
6. March, R.E., Hughes, R.J.: Quadrupole Storage Mass Spectrometry, p. 471. Wiley, New York (1989)
7. Tolmachev, A.V., Udseth, H.R., Smith, R.D.: Charge capacity limitations of radio frequency ion guides in their use for improved ion accumulation and trapping in mass spectrometry. Anal. Chem. **72**, 970–978 (2000)
8. March, R.E., Todd, J.F.J.: Quadrupole Ion Trap Mass Spectrometry, 2nd edn. Wiley, Hoboken (2005)
9. Guan, S.H., Marshall, A.G.: Equilibrium space-charge distribution in a quadrupole ion-trap. J. Am. Soc. Mass Spectrom. **5**, 64–71 (1994)
10. Xiong, X.C., Xu, W., Fang, X., Deng, Y.L., Ouyang, Z.: Accelerated simulation study of space charge effects in quadrupole ion traps using GPU techniques. J. Am. Soc. Mass Spectrom. **23**, 1799–1807 (2012)
11. Li, G.Z., Guan, S.H., Marshall, A.G.: Comparison of equilibrium ion density distribution and trapping force in Penning, Paul, and combined ion traps. J. Am. Soc. Mass Spectrom. **9**, 473–481 (1998)
12. Vedel, F., Andre, J.: Influence of space charge on the computed statistical properties of stored ions cooled by a buffer gas in a quadrupole rf trap. Phys. Rev. A **29**, 2098 (1984)
13. Todd, J.F.J., Waldren, R.M., Freer, D.A., Turner, R.B.: The quadrupole ion store (QUISTOR) 10. Space-charge and ion stability b on the theoretical distribution and density of stored charge in rf quadrupole fields. Int. J. Mass Spectrom. Ion Process. **35**, 107–150 (1980)
14. Todd, J.F.J., Waldren, R.M., Mather, R.E.: The quadrupole ion store (QUISTOR) 9. Space-charge and ion stability—a theoretical background and experimental results. Int. J. Mass Spectrom. Ion. Process. **34**, 325–349 (1980)
15. Cooks, R.G.: Special feature: Historical. Collision-induced dissociation: readings and commentary. J. Mass Spectrom. **30**, 1215–1221 (1995)
16. Qiao, H., Gao, C., Mao, D.M., Konenkov, N., Douglas, D.J.: Space-charge effects with mass-selective axial ejection from a linear quadrupole ion trap. Rapid Commun. Mass Spectrom. **25**, 3509–3520 (2011)
17. Cox, K.A., Cleven, C.D., Cooks, R.G.: Mass shifts and local space charge effects observed in the quadrupole ion trap at higher resolution. Int. J. Mass Spectrom. Ion Process. **144**, 47–65 (1995)

18. Douglas, D.J., Frank, A.J., Mao, D.: Linear ion traps in mass spectrometry. Mass Spectrom. Rev. **24**, 1–29 (2005)
19. Plass, W.R., Li, H., Cooks, R.G.: Theory, simulation, and measurement of chemical mass shifts in rf quadrupole ion traps. Int. J. Mass Spectrom. **228**, 237–267 (2003)
20. Schwartz, J.C., Senko, M.W., Syka, J.E.P.: A two-dimensional quadrupole ion trap mass spectrometer. J. Am. Soc. Mass Spectrom. **13**, 659–669 (2002)
21. Cleven, C.D., Cooks, R.G., Garrett, A.W., Nogar, N.S., Hemberger, P.H.: Radial distributions and ejection times of molecular ions in an ion trap mass spectrometer: a laser tomography study of effects of ion density and molecular type. J. Phys. Chem. **100**, 40–46 (1996)
22. Plass, W.R., Gill, L.A., Bui, H.A., Cooks, R.G.: Ion mobility measurement by DC tomography in an rf quadrupole ion trap. J. Phys. Chem. A **104**, 5059–5065 (2000)
23. Hager, J.W.: A new linear ion trap mass spectrometer. Rapid Commun. Mass Spectrom. **16**, 512–526 (2002)
24. Nikolaev, E.N., Heeren, R.M.A., Popov, A.M., Pozdneev, A.V., Chingin, K.S.: Realistic modeling of ion cloud motion in a Fourier transform ion cyclotron resonance cell by use of a particle-in-cell approach. Rapid Commun. Mass Spectrom. **21**, 3527 (2007)
25. Ledford, E.B., Rempel, D.L., Gross, M.L.: Space charge effects in Fourier transform mass spectrometry. II. Mass calibration. Anal. Chem. **56**, 2744–2748 (1984)
26. Amster, I.J.: Fourier transform mass spectrometry. J. Mass Spectrom. **31**, 1325–1337 (1996)
27. Comisarow, M.B., Marshall, A.G.: Frequency-sweep Fourier transform ion cyclotron resonance spectroscopy. Chem. Phys. Lett. **26**, 489–490 (1974)
28. Comisarow, M.B., Marshall, A.G.: Fourier transform ion cyclotron resonance spectroscopy. Chem. Phys. Lett. **25**, 282–283 (1974)
29. Jeffries, J.B., Barlow, S.E., Dunn, G.H.: Theory of space-charge shift of ion cyclotron resonance frequencies. Int. J. Mass Spectrom. Ion Process. **54**, 169–187 (1983)
30. Nikolaev, E.N., Miluchihin, N.V., Inoue, M.: Evolution of an ion cloud in a Fourier transform ion cyclotron resonance mass spectrometer during signal detection: its influence on spectral line shape and position. Int. J. Mass Spectrom. Ion Process. **148**, 145–157 (1995)
31. Leach III, F.E., Kharchenko, A., Heeren, R., Nikolaev, E., Amster, I.J.: Comparison of particle-in-cell simulations with experimentally observed frequency shifts between ions of the same mass-to-charge in Fourier transform ion cyclotron resonance mass spectrometry. J. Am. Soc. Mass Spectrom. **21**, 203–208 (2010)
32. Hu, Q., Noll, R.J., Li, H., Makarov, A., Hardman, M., Cooks, R.G.: The Orbitrap: a new mass spectrometer. J. Mass Spectrom. **40**, 430–443 (2005)
33. Ding, L., Sudakov, M., Brancia, F.L., Giles, R., Kumashiro, S.: A digital ion trap mass spectrometer coupled with atmospheric pressure ion sources. J. Mass Spectrom. **39**, 471–484 (2004)
34. Sevugarajan, S., Menon, A.G.: Frequency perturbation in nonlinear Paul traps: a simulation study of the effect of geometric aberration, space charge, dipolar excitation, and damping on ion axial secular frequency. Int. J. Mass Spectrom. **197**, 263–278 (2000)
35. Wang, Y.Z., Huang, Z.J., Jiang, Y., Xiong, X.C., Deng, Y.L., Fang, X., Xu, W.: The coupling effects of hexapole and octopole fields in quadrupole ion traps: a theoretical study. J. Mass Spectrom. **48**, 937–944 (2013)
36. Mickens, R.E.: A generalization of the method of harmonic-balance. J. Sound Vib **111**, 515–518 (1986)
37. Guo, D., Wang, Y.Z., Xiong, X.C., Zhang, H., Zhang, X.H., Yuan, T., Fang, X., Xu, W.: Space charge induced nonlinear effects in quadrupole ion traps. J. Am. Soc. Mass Spectrom. **25**, 498–508 (2014)
38. Londry, F.A., Hager, J.W.: Mass selective axial ion ejection from a linear quadrupole ion trap. J. Am. Soc. Mass Spectrom. **14**, 1130–1147 (2003)
39. Wang, Y., Zhang, X., Zhai, Y., Jiang, Y., Fang, X., Zhou, M., Deng, Y., Xu, W.: Mass selective ion transfer and accumulation in ion trap arrays. Anal. Chem. **86**, 10164–10170 (2014)
40. Xu, W., Chappell, W.J., Ouyang, Z.: Modeling of ion transient response to dipolar AC excitation in a quadrupole ion trap. Int. J. Mass Spectrom. **308**, 49–55 (2011)
41. Parks, J.H., Szoke, A.: Simulation of collisional relaxation of trapped ion clouds in the presence of space-charge fields. J. Chem. Phys. **103**, 1422–1439 (1995)
42. Grinfeld, D.E., Kopaev, I.A., Makarov, A.A., Monastyrskiy, M.A.: Equilibrium ion distribution modeling in rf ion traps and guides with regard to Coulomb effects. Nucl. Instrum. Methods Phy. Res. A **645**, 141–145 (2011)